

Exploring the nucleon structure through GPDs and TDAs in hard exclusive processes

B. Pire¹, K. Semenov-Tian-Shansky^{1,2}, L. Szymanowski³ and J. Wagner³

¹ CPhT, École Polytechnique, CNRS, 91128 Palaiseau, France

² LPT, Université Paris-Sud, CNRS, 91405 Orsay, France

³ Sołtan Institute for Nuclear Studies, Hoża 69, 00-681 Warsaw, Poland

E-mail: pire@cpht.polytechnique.fr

Abstract. Generalized Parton Distributions (GPDs) offer a new way to access the quark and gluon nucleon structure. We review recent progress in this domain, emphasizing the need to supplement the experimental study of deeply virtual Compton scattering by its crossed version, timelike Compton scattering. We also describe the extension of the GPD concept to three quark operators and the relevance of their nucleon to meson matrix elements, namely the transition distribution amplitudes (TDAs) which factorize in backward meson electroproduction and related processes. We discuss the main properties of the TDAs.

1. Introduction

The study of the internal structure of the nucleon has been the subject of many developments in the past decades and the concept of generalized parton distributions has allowed a breakthrough in the 3 dimensional description of the quark and gluon content of hadrons. Hard exclusive reactions have been demonstrated to allow to probe the quark and gluon content of protons and heavier nuclei.

In this short review, we concentrate on two timely items: firstly, we emphasize the complementarity of timelike and spacelike studies of hard exclusive processes, taking as an example the case of timelike Compton scattering (TCS) where data at medium energy should be available at JLab@12 GeV, supplemented by higher energy data thanks both to a forthcoming electron-ion collider and to the study of ultraperipheral collisions at the LHC. Secondly, we show how the backward region of deeply virtual meson electroproduction processes may be described in a factorized way, with the necessary extension of the GPD concept to three quark operators and their nucleon to meson matrix elements, the transition distribution amplitudes (TDAs).

2. Timelike vs spacelike DVCS

A considerable amount of theoretical and experimental work has been devoted to the study of deeply virtual Compton scattering (DVCS), i.e., $\gamma^*p \rightarrow \gamma p$, an exclusive reaction where generalized parton distributions (GPDs) factorize from perturbatively calculable coefficient functions, when the virtuality of the incoming photon is large enough [1]. It is now recognized that the measurement of GPDs should contribute in a decisive way to our understanding of how quarks and gluons assemble into hadrons [2]. In particular, the transverse location of quarks and

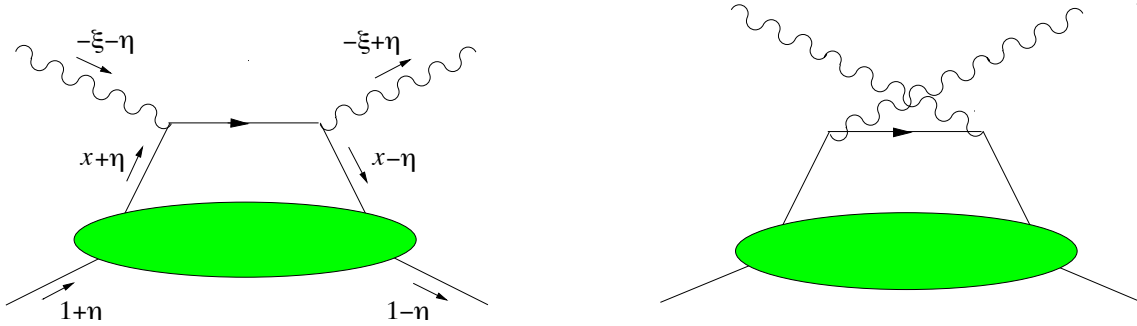


Figure 1. Handbag diagrams for the Compton process in the scaling limit. The plus-momentum fractions x , ξ , η refer to the average proton momentum $\frac{1}{2}(p + p')$. In the DVCS case, $\xi = \eta$ while in the TCS case $\xi = -\eta$.

gluons become experimentally measurable via the transverse momentum dependence of GPDs [3]. Results on DVCS [4] obtained at HERA and JLab already allow to get a rough idea of some of the GPDs (more precisely of the Compton form factors) in a restricted but interesting kinematical domain [5]. An extended research program at JLab@12 GeV and Compass is now proposed to go beyond this first set of analysis. This will involve taking into account next to leading order in α_s and next to leading twist contributions [6].

The physical process where to observe the inverse reaction, timelike Compton scattering (TCS) [7],

$$\gamma(q)N(p) \rightarrow \gamma^*(q')N(p') \quad (1)$$

is the exclusive photoproduction of a heavy lepton pair, $\gamma N \rightarrow \mu^+\mu^- N$ or $\gamma N \rightarrow e^+e^- N$, at small $t = (p' - p)^2$ and large *timelike* final state lepton pair squared mass $q'^2 = Q'^2$; TCS shares many features with DVCS. The generalized Bjorken variable in that case is $\tau = Q'^2/s$ with $s = (p + q)^2$. One also defines $\Delta = p' - p$ ($t = \Delta^2$) and the skewness variable η as

$$\eta = -\frac{(q - q') \cdot (q + q')}{(p + p') \cdot (q + q')} \approx \frac{Q'^2}{2s - Q'^2} = \frac{\tau}{(2 - \tau)}.$$

At the Born order, the TCS amplitude is described by the handbag diagrams of Fig. 1. As in the case of DVCS, purely electromagnetic mechanism where the lepton pair is produced through the Bethe-Heitler (BH) subprocess $\gamma(q)\gamma^*(\Delta) \rightarrow \ell^+\ell^-$, contributes at the amplitude level. This amplitude is completely calculable in QED provided one knows the nucleon form factors at small $\Delta^2 = t$. This process has a very peculiar angular dependence and overdominates the TCS process if one blindly integrates over the final phase space. One may however choose kinematics where the amplitudes of the two processes are of the same order of magnitude, and either subtract the well-known Bethe-Heitler process or use specific observables sensitive to the interference of the two amplitudes. Finally some kinematical cuts may allow to decrease sufficiently the Bethe Heitler contribution.

The kinematics of the $\gamma(q)N(p) \rightarrow \ell^-(k)\ell^+(k')N(p')$ process is shown in Fig.2. In the $\ell^+\ell^-$ center of mass system, one introduces the polar and azimuthal angles θ and φ of \vec{k} , with reference to a coordinate system with 3-axis along $-\vec{p}'$ and 1- and 2-axes such that \vec{p} lies in the 1-3 plane and has a positive 1-component. Since the amplitudes for the Compton and Bethe-Heitler processes transform with opposite signs under reversal of the lepton charge, the interference term between TCS and BH is odd under exchange of the ℓ^+ and ℓ^- momenta. It is thus possible to project out the interference term through a clever use of the angular distribution of the lepton pair. The interference part of the cross-section for $\gamma p \rightarrow \ell^+\ell^- p$ with unpolarized protons and

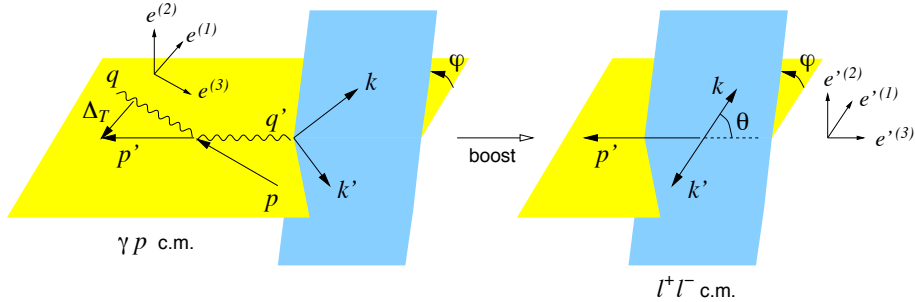


Figure 2. Kinematical variables and coordinate axes in the γp and $\ell^+ \ell^-$ c.m. frames.

photons has a characteristic (θ, φ) dependence given by (see details in [10])

$$\frac{d\sigma_{INT}}{dQ^2 dt d\cos\theta d\varphi} = -\frac{\alpha_{em}^3}{4\pi s^2} \frac{1}{-t} \frac{M}{Q'} \frac{1}{\tau\sqrt{1-\tau}} \cos\varphi \frac{1+\cos^2\theta}{\sin\theta} \text{Re } \mathcal{M},$$

with

$$\mathcal{M} = \frac{2\sqrt{t_0-t}}{M} \frac{1-\eta}{1+\eta} \left[F_1 \mathcal{H}_1 - \eta(F_1 + F_2) \tilde{\mathcal{H}}_1 - \frac{t}{4M^2} F_2 \mathcal{E}_1 \right], \quad (2)$$

where $-t_0 = 4\eta^2 M^2 / (1-\eta^2)$, \mathcal{H} , $\tilde{\mathcal{H}}$, \mathcal{E} are Compton form factors and F_1, F_2 are the nucleon Dirac and Pauli form factors. With the integration limits symmetric about $\theta = \pi/2$ the interference term changes sign under $\varphi \rightarrow \pi + \varphi$ due to charge conjugation, whereas the TCS and BH cross sections do not. One may thus extract the Compton amplitude through a study of $\int_0^{2\pi} d\phi \cos\phi \frac{d\sigma}{d\phi}$.

This program has not yet been experimentally successful [8] due to the existing limited quasi real photon flux in the appropriate kinematical domain both at JLab and HERA. This will be much improved with the JLab@12 GeV program, both in Hall B [9] and in Hall D. These experiments will enable to test the universality of GPDs extracted from DVCS and from TCS, provided NLO corrections are taken into account. Experiments at higher energies, e.g. in ultraperipheral collisions at RHIC and LHC [10] or in a future electron-ion collider [11], may even become sensitive to gluon GPDs which enter the amplitude only at NLO level. TCS and DVCS amplitudes are identical (up to a complex conjugation) at lowest order in α_S but differ at next to leading order, in particular because of the quite different analytic structure of these reactions. Indeed the production of a timelike photon enables the production of intermediate states in some channels which were kinematically forbidden in the DVCS case.

2.1. LO estimates in ultraperipheral collisions

We estimated [10] the different contributions to the lepton pair cross section for ultraperipheral collisions at the LHC. Since the cross sections decrease rapidly with Q^2 , we are interested in the kinematics of moderate Q^2 , say a few GeV^2 , and large energy, thus very small values of η . Note however that for a given proton energy the photon flux is higher at smaller photon energy.

In Fig. 3 we show the interference contribution to the cross section in comparison to the Bethe Heitler and Compton processes, for various values of photon proton energy squared $s = 10^7 \text{ GeV}^2, 10^5 \text{ GeV}^2$. We observe that for larger energies the Compton process dominates, whereas for $s = 10^5 \text{ GeV}^2$ all contributions are comparable.

Our leading order estimate shows that the factorization scale dependence of the amplitudes is quite high. This fact demands the understanding of higher order contributions with the hope that they will stabilize this scale dependence.

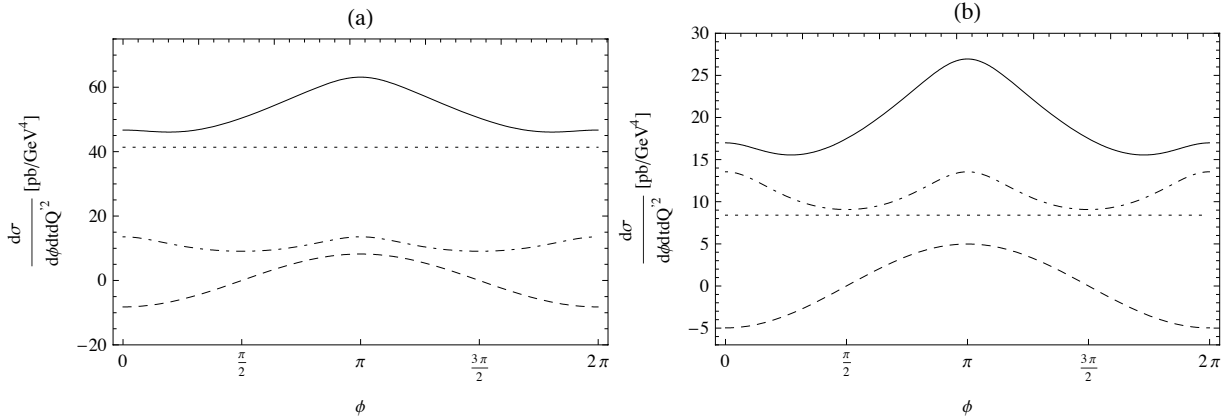


Figure 3. The differential cross sections (solid lines) for $t = -0.2 \text{ GeV}^2$, $Q'^2 = 5 \text{ GeV}^2$ integrated over $\theta = [\pi/4, 3\pi/4]$, as a function of φ , for $s = 10^7 \text{ GeV}^2$ (a), $s = 10^5 \text{ GeV}^2$ (b) with $\mu_F^2 = 5 \text{ GeV}^2$. We also display the Compton (dotted), Bethe-Heitler (dash-dotted) and Interference (dashed) contributions.

2.2. NLO corrections

Our calculations [12] of NLO corrections show important differences between the coefficient functions describing the TCS case and those describing DVCS. First, the $p^2 + i\varepsilon$ prescription for propagators turns into a $\eta \rightarrow \eta + i\varepsilon$, rather than a $\eta \rightarrow \eta - i\varepsilon$ as in the DVCS case. The second difference is the presence of minus signs under the logarithms, which produce additional terms. Particularly $\log^2(-2 - i\varepsilon)$ present in the TCS result may produce correction much bigger than the corresponding $\log^2(2)$ in the DVCS case. Another important difference between the DVCS and TCS amplitudes appear in their imaginary part, which is present only in the DGLAP region for DVCS, while it is present in both DGLAP and ERBL regions for TCS. Defining the quark and gluon coefficient functions as

$$T^q = C_0^q + C_1^q + \frac{1}{2} \log\left(\frac{|Q^2|}{\mu_F^2}\right) C_{coll}^q \quad ; \quad T^g = C_1^g + \frac{1}{2} \log\left(\frac{|Q^2|}{\mu_F^2}\right) C_{coll}^g ,$$

where C_0^q is the Born order coefficient function and μ_F is the factorization scale. C_{coll}^q and C_{coll}^g are directly related to the evolution equation kernels.

To discuss the difference of the coefficient functions $C_{1(TCS)}^q - C_{1(DVCS)}^q$ and present the magnitude of corrections we define the following ratio:

$$R^q = \frac{C_1^q + \frac{1}{2} \log\left(\frac{|Q^2|}{\mu_F^2}\right) \cdot C_{coll}^q}{C_0^q} \quad (3)$$

of the NLO quark correction to the coefficient function, to the Born level one. Let us restrict us to the factorization scale choice $\mu_F^2 = |Q^2|$. On Fig. 4 we show the real and imaginary parts of the ratio R^q in timelike and spacelike Compton Scattering as a function of x in the ERBL (left) and DGLAP (right) region for $\eta = 0.3$. We fix $\alpha_s = 0.25$ and restrict the plots to the positive x region, as the coefficient functions are antisymmetric in that variable. We see that in the TCS case, as the coefficient functions are antisymmetric in that variable. We see that in the TCS case, the imaginary part of the amplitude is present in both the ERBL and DGLAP regions, contrarily to the DVCS case, where it exists only in the DGLAP region. The magnitudes of these NLO coefficient functions are not small and neither is the difference of the coefficient functions $C_{1(TCS)}^q - C_{1(DVCS)}^q$. The conclusion is that extracting the universal GPDs from both TCS and DVCS reactions requires much care.

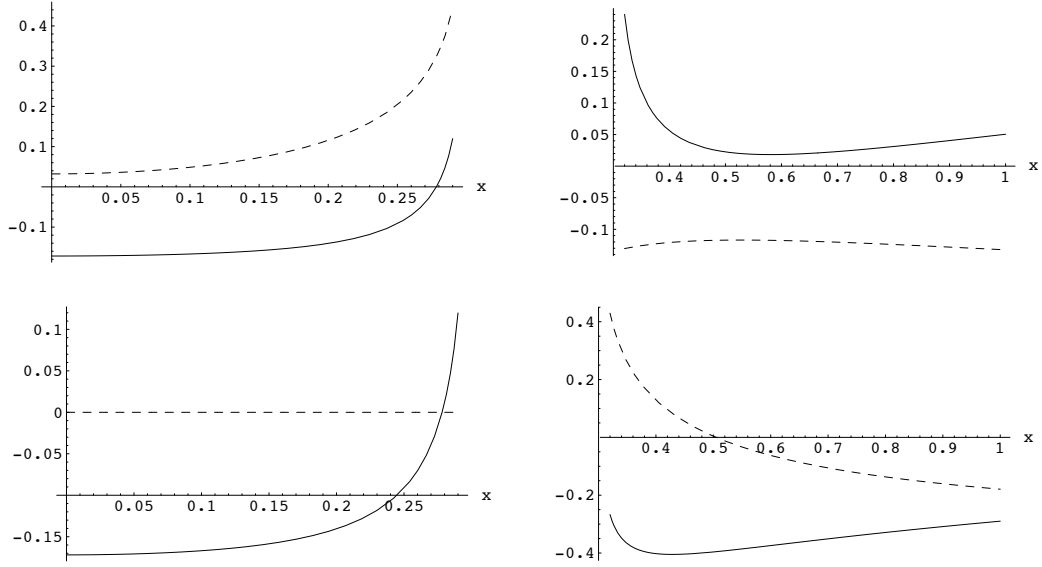


Figure 4. Real (solid line) and imaginary (dashed line) part of the ratio R^q of the NLO quark coefficient function to the Born term in Timelike Compton Scattering (up) and Deeply Virtual Compton Scattering (down) as a function of x in the ERBL (left) and DGLAP (right) region for $\eta = 0.3$, for $\mu_F^2 = |Q^2|$.

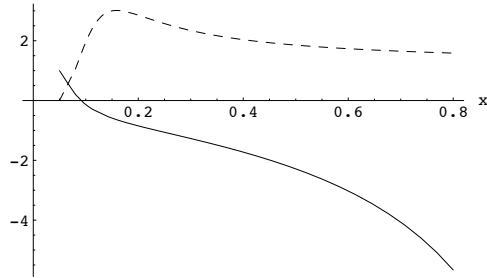


Figure 5. Ratio of the real (solid line) and imaginary (dashed line) part of the NLO gluon coefficient function in TCS to the same quantity in DVCS as a function of x in the DGLAP region for $\eta = 0.05$ for $\mu_F^2 = |Q^2|$.

Let us now briefly comment on the gluon coefficient functions. The real parts of the gluon contribution are equal for DVCS and TCS in the ERBL region. The differences between TCS and DVCS emerges in the ERBL region through the imaginary part of the coefficient function which is non zero only for the TCS case and is of the order of the real part. In Fig. 5 we plot the ratio $\frac{C_{1(TCS)}^g}{C_{1(DVCS)}^g}$ of the NLO gluon correction to the hard scattering amplitude in TCS to the same quantity in the DVCS in the DGLAP region for $\eta = 0.05$.

More phenomenological studies need now to be performed, by convoluting the coefficient functions to realistic quark and gluon GPDs and calculating the relevant observables in various kinematical domains. We are now progressing on these points.

3. On Transition Distribution Amplitudes

Hadronic matrix elements of non-local light-cone operators are the conventional non-perturbative objects which arise in the description of hard exclusive electroproduction reactions within the collinear factorization approach. The factorization theorem for backward DVCS [13] and for hard exclusive backward meson electroproduction argued in [14, 15] lead to the introduction of baryon to meson transition distribution amplitudes (TDAs), non diagonal matrix elements of light-cone three quark operators

$$\widehat{O}_{\rho\tau\chi}^{\alpha\beta\gamma}(z_1, z_2, z_3) = \varepsilon_{c_1c_2c_3} \Psi_{\rho}^{c_1\alpha}(z_1) \Psi_{\tau}^{c_2\beta}(z_2) \Psi_{\chi}^{c_3\gamma}(z_3) \quad (4)$$

between baryon and meson states. In (4) α, β, γ stand for quark flavor indices; ρ, τ and χ denote the Dirac indices and $c_{1,2,3}$ are indices of the color group. If one adopts the light-cone gauge $A^+ = 0$, the gauge link is equal to unity and may be omitted in the definition of the operator (4). Baryon to meson TDAs extend the concept of generalized parton distributions. They appear as a building block in the collinear factorized description of amplitudes for a class of hard exclusive reactions prominent examples being hard exclusive pion electroproduction off a nucleon in the backward region and baryon-antibaryon annihilation into a pion and a lepton pair [16].

πN TDAs appear in the description of backward electroproduction of a pion on a nucleon target (see Fig.6 a). In terms of angles, in the γ^*p center of momentum (CM) frame, the angle between the γ^* and the pion, θ_{π}^* , is close to 180° . We then have $|u| \ll s$ and $t \simeq -(s + Q^2)$, in contrast to the fixed angle regime $u \simeq t \simeq -(s + Q^2)/2$ ($\theta_{\pi}^* \simeq 90^\circ$) and the forward (GPD) one $|t| \ll s$ and $u \simeq -(s + Q^2)$ ($\theta_{\pi}^* \simeq 0^\circ$).

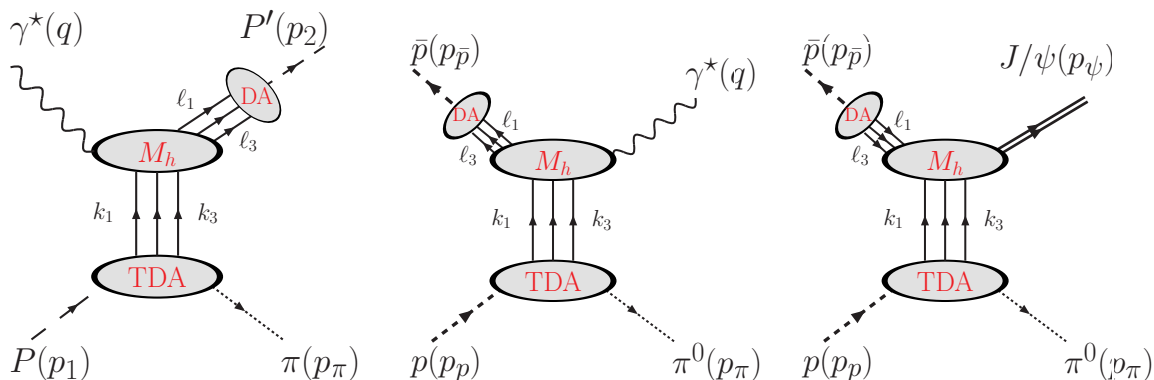


Figure 6. Illustration of the factorisation for three exclusive reactions involving the TDAs.

The TDAs appear also in similar electroproduction processes such as $ep \rightarrow e(p, \Delta^+) (\eta, \rho^0)$, $ep \rightarrow e(n, \Delta) (\pi^+, \rho^+)$, $ep \rightarrow e \Delta^{++} (\pi^-, \rho^-)$. Those processes have already been analysed, at backward angles, at JLab in the resonance region, i.e. $\sqrt{s_{\gamma^*p}} = W < 1.8$ GeV, in order to study the baryonic transition form factors in the π channel or in the η channel. Data are being extracted in some channels above the resonance region. The number of events seems to be large enough to expect to get cross section measurements for $\Delta_T^2 < 1$ GeV², which is the region described in terms of TDAs. The HERMES analysis for forward electroproduction may also be extended to larger values of $-t$. It has to be noted though that present studies are limited to Q^2 of order a few GeV², which gives no guarantee to reach the TDA regime yet. Higher- Q^2 data may be obtained at JLab-12 GeV and in muoproduction at Compass within the next few years.

Crossed reactions in proton-antiproton annihilation (e.g. with PANDA at GSI-FAIR [19]), with time-like photons (i.e. di-leptons) and a pion (see Fig.6 b) also involve TDAs both for small

$t = (p_p - p_{\pi^0})^2$ and $u = (p_{\bar{p}} - p_{\pi^0})^2$. In the latter case, the TDAs for a transition between the anti-proton and the pion are probed. One can also study similar reactions with other mesons than a pion, e.g. $\bar{p}p \rightarrow \gamma^* (\eta, \rho^0)$, or on a different target than proton $\bar{p}N \rightarrow \gamma^*\pi$. Finally, one may also consider associated J/ψ production with a pion $\bar{p}p \rightarrow J/\psi \pi^0$ (see Fig.6 c) or another meson $\bar{p}p \rightarrow J/\psi (\eta, \rho^0)$, which involve the *same* TDAs as with an off-shell photon or in backward electroproduction. They will serve as very strong tests of the universality of TDAs in different processes.

The first application of baryonic TDAs was centered on backward electroproduction of a pion [17]. In that case, the hard contribution which consists in the scattering of the hard photon with three quarks is known at leading order. Extrapolating the limiting value of πN TDAs obtained from the soft pion theorems, we obtained a first evaluation of the unpolarised cross section for backward electroproduction in the region of large- ξ . This estimate, which is unfortunately reliable only in a very restricted kinematical domain (large- ξ), shows an interesting sensitivity to the underlying model of the proton DA. This study has been extended to hard exclusive production of a $\gamma^*\pi^0$ pair in $\bar{p}p$ annihilation at GSI-FAIR [18].

πN TDAs are non-perturbative objects governed by long distance dynamics. In accordance with the usual logic of the collinear factorization approach πN TDAs have well established renormalization group properties. The evolution properties of the three quark non-local operator on the light-cone were extensively studied in the literature for the case of matrix elements between a baryon and the vacuum known as baryon distribution amplitudes (DAs). Since TDAs involve the same operator its evolution determines the factorization scale dependence of TDAs [16]. We derived [20] a spectral representation for the πN TDAs, and introduced the notion of quadruple distributions which enable to generalize Radyushkin's factorized Ansatz from the GPD case to the TDA case. Lorentz invariance results in a polynomiality property of the Mellin moments of TDAs in the longitudinal momentum fractions.

The detailed account of isospin and permutation symmetries [21] provides a unified description of all isotopic channels in terms of eight independent πN TDAs. These general constraints derived should be satisfied by any realistic model of TDAs. The crossing relation between πN TDAs and GDAs leads to a soft pion theorem for isospin- $\frac{1}{2}$ and isospin- $\frac{3}{2}$ πN TDAs, which helps to derive normalization conditions for πN TDAs. A simple resonance exchange model considering nucleon and $\Delta(1232)$ exchanges in isospin- $\frac{1}{2}$ and isospin- $\frac{3}{2}$ channels respectively allows to approximate πN TDAs in the ERBL region [21]. Nucleon exchange may be considered as a pure D -term contribution generating the highest power monomials of ξ of the Mellin moments in the longitudinal momentum fractions, complementary to the spectral representation for TDAs in terms of quadruple distributions.

Backward hard-exclusive reactions thus open new windows in the understanding of hadronic physics in the framework of the collinear-factorization approach of QCD. To extract reliable precise information on the baryon to meson transition distribution amplitudes from an incomplete set of observables such as cross sections and asymmetries, one needs to develop realistic models for the TDAs. Nonperturbative techniques such as lattice simulations need to be adapted to this problem. Three approaches – the soft pion theorem, the pion-cloud model [22] and the spectral representation – are being explored and first cross-section evaluations in the whole kinematical domain covered by the TDA factorisation should be available soon.

The 12 GeV JLab upgrade and the start-up of GSI-FAIR hopefully will bring us the necessary experimental information to test the model-independent predictions of the TDA factorisation and then to check specific predictions from different TDA models potentially connected to the more fundamental quantity of the hadronic realm.

Acknowledgments

We acknowledge useful discussions with Grzegorz Grzelak, Jean-Philippe Lansberg, Paweł Nadel-Turoński and Samuel Wallon. This work was supported by the French-Polish Scientific Agreement Polonium and by the Consortium Physique des Deux Infinis (P2I).

References

- [1] Müller D *et al.* 1994 *Fortsch. Phys.* **42** 101
Ji X 1997 *Phys. Rev. Lett.* **78** 610
Radyushkin A V 1997 *Phys. Rev. D* **56** 5524
Collins J C and Freund A 1999 *Phys. Rev. D* **59** 074009
- [2] Diehl M 2003 *Phys. Rept.* **388** 41
Belitsky A V and Radyushkin A V 2005 *Phys. Rept.* **418** 1
- [3] Burkardt M 2000 *Phys. Rev. D* **62** 071503;
Ralston JP and Pire B 2002 *Phys. Rev. D* **66** 111501 ;
Diehl M 2002 *Eur. Phys. J. C* **25** 223 .
- [4] A. Airapetian *et al.* [HERMES Collaboration] 2001 *Phys. Rev. Lett.* **87** 182001 ;
Munoz Camacho C *et al.* [Jefferson Lab Hall A Collaboration] 2006 *Phys. Rev. Lett.* **97** 262002;
Chekanov S *et al.* [ZEUS Collaboration] 2003 *Phys. Lett. B* **573** 46;
Aktas A *et al.* [H1 Collaboration] 2005 *Eur. Phys. J. C* **44** 1 ;
Stepanyan S *et al.* [CLAS Collaboration] 2001 *Phys. Rev. Lett.* **87** 182002 .
- [5] Kumericki K, Mueller D and Passek-Kumericki K 2008 *Nucl. Phys. B* **794** 244 ;
Guidal M and Moutarde H 2009 *Eur. Phys. J. A* **42** 71 ;
Moutarde H 2009 *Phys. Rev. D* **79** 094021 .
- [6] Anikin IV, Pire B and Teryaev OV 2000 *Phys. Rev. D* **62** 071501 ;
Belitsky AV *et al.* 2001 *Phys. Lett. B* **510** 117 ;
Belitsky AV and Mueller D 2010 *Phys. Rev. D* **82** 074010 .
- [7] Berger ER, Diehl M and Pire B 2002 *Eur. Phys. J. C* **23** 675.
- [8] Nadel-Turoński P *et al.* 2009 *AIP Conf. Proc.* **1182** 843.
- [9] Albayrak I *et al.* e^+e^- pair production with CLAS12 at 11 GeV, CLAS letter of intent (2011).
- [10] Pire B, Szymanowski L and Wagner J 2009 *Phys. Rev. D* **79** 014010 , *Nucl. Phys. Proc. Suppl.* **179-180** 232 and *Acta Phys. Polon. Supp.* **2**, 373 .
- [11] Boer D *et al.* 2011 Gluons and the quark sea at high energies: Distributions, polarization, tomography *Preprint* arXiv:1108.1713 [nucl-th].
- [12] Pire B, Szymanowski L and Wagner J 2011 *Phys. Rev. D* **83**, 034009 .
- [13] Pire B and Szymanowski L 2005 *Phys. Rev. D* **71** 111501 ;
Lansberg JP, Pire B and Szymanowski L 2006 *Phys. Rev. D* **73** 074014 .
- [14] Frankfurt LL *et al.* 1999 *Phys. Rev. D* **60** 014010.
- [15] Frankfurt LL *et al.* 2002 Novel hard semiexclusive processes and color singlet clusters in hadrons *Preprint* hep-ph/0211263.
- [16] Pire B and Szymanowski L 2005 *Phys. Lett. B* **622** 83
- [17] Lansberg JP, Pire B and Szymanowski L 2007 *Phys. Rev. D* **75** 074004 [Erratum-ibid. D **77** 019902].
- [18] Lansberg JP, Pire B and Szymanowski L 2007 *Phys. Rev. D* **76** 111502 .
- [19] Lutz MF *et al.* [The PANDA Collaboration] 2009 Physics Performance Report for PANDA: Strong Interaction Studies with Antiprotons *Preprint* arXiv:0903.3905 [hep-ex].
- [20] Pire B, Semenov-Tian-Shansky K and Szymanowski L 2010 *Phys. Rev. D* **82** 094030 ,
Pire B, Semenov-Tian-Shansky K and Szymanowski L 2011 *AIP Conf. Proc.* **1350** 237.
- [21] Pire B, Semenov-Tian-Shansky K and Szymanowski L 2011 πN transition distribution amplitudes: their symmetries and constraints from chiral dynamics *Preprint* arXiv:1106.1851 [hep-ph].
- [22] Pasquini B, Pincetti M and Boffi S 2009 *Phys. Rev. D* **80** 014017 .